

Bremsstrahlung and Pair Creation: Suppression Mechanisms and How They Affect EHE Air Showers

Spencer R. Klein

Lawrence Berkeley National Laboratory, Berkeley, CA, 94720

Abstract. Most calculations of air shower development have been based on the Bethe-Heitler cross sections for bremsstrahlung and pair production. However, for energetic enough particles, a number of different external factors can reduce these cross sections drastically, slowing shower development and lengthening the showers. Four mechanisms that can suppress bremsstrahlung and pair production cross sections are discussed, and their effect on extremely high energy air showers considered. Besides lengthening the showers, these mechanisms greatly increase the importance of fluctuations in shower development, and can increase the angular spreading of showers.

Presented at the Workshop on
“*Observing Giant Cosmic Ray Airshowers for $> 10^{20}$ eV Particles from Space*”
November 13-15, 1997, College Park, MD

INTRODUCTION

The electromagnetic portion of high energy air showers is governed by bremsstrahlung and pair production. Although the formulae for these process have been around for over 60 years, it is not well known that, in many situations, these formulae can be very wrong. The medium in which the bremsstrahlung or pair production occurs can drastically affect the cross sections. This contribution will discuss four different ways in which the medium can reduce the bremsstrahlung and pair creation cross sections.

These suppression mechanisms can affect air showers by increasing the effective radiation length, lengthening the showers, and moving the position of the shower maximum deeper into the atmosphere. For ground based arrays like the proposed Auger Observatory, even a small change in the depth of shower max can affect the energy hitting the ground, especially for non-vertical showers where shower maximum is considerably above ground level. Air fluorescence detectors like Flys Eye

and the proposed OWL can measure the shower profile, and so their energy measurement would be less affected by unforeseen changes in the shower development. However, a change in the position of shower maximum can affect measurements of the composition of the highest energy cosmic rays. Moreover, these mechanisms will drastically reduce the number of particles in the early stages of the shower, changing the shower development profile.

I BREMSSTRAHLUNG AND PAIR PRODUCTION SUPPRESSION MECHANISMS

Suppression mechanisms for bremsstrahlung and pair production are possible because of the unusual kinematics in these processes. For ultrarelativistic particles, the momentum transfer between the radiating electron or converting photon and the target nucleus is very small, especially in the longitudinal direction [1]. For bremsstrahlung where $E \gg m$,

$$q_{\parallel} = p_e - p'_e - k/c \quad (1)$$

$$= \sqrt{(E/c)^2 - (mc)^2} - \sqrt{((E-k)/c)^2 - (mc)^2} - k/c = \frac{m^2 c^3 k}{2E(E-k)} \quad (2)$$

where p_e and p'_e are the electron momenta before and after the interaction respectively, k is the photon energy, m is the electron mass and $\gamma = E/m$. For ultrarelativistic electrons, q_{\parallel} can be very small. For example, for a 1 EeV electron emitting a 100 PeV photon, $q_{\parallel} = 10^{-9} \text{eV}/c$. Because q_{\parallel} is so small, by the uncertainty principle, it must take place over a long distance, known as the formation length:

$$l_{f0} = \frac{\hbar}{q_{\parallel}} = \frac{2\hbar E(E-k)}{m^2 c^3 k}. \quad (3)$$

For the above example, l_{f0} is 200 meters; for a 1 PeV photon from the same electron, l_{f0} rises to 20 km. This distance is the distance required for the electron and photon to separate to become distinct particles. It is also the path length over which the emission amplitude adds coherently to produce the emission probability. If something happens to the electron or nascent photon while it is traversing the formation zone, then the coherence can be disrupted, reducing the effective formation length and hence the emission probability. Even weak forces, acting over a long formation length, can be strong enough to destroy the coherence required for emission. The mechanisms discussed here work by disrupting the electron or photon, reducing the effective formation length.

A Multiple Scattering (The LPM Effect)

Multiple scattering can cause disruption by changing the electron trajectory. If, taken over l_{f0} , the electron multiple scatters by an angle larger than the typical

bremstrahlung emission angle $1/\gamma$, then emission can be suppressed [1].

The reduction can be calculated by considering the effect multiple scattering has on q_{\parallel} ; as the electron changes direction, it's forward velocity is reduced, and, with it, producing a change in q_{\parallel} . This can be modelled by dividing the multiple scattering evenly between p_e and p'_e . Then,

$$q_{\parallel} = \sqrt{(E \cos \theta_{MS/2}/c)^2 - (mc)^2} - \sqrt{((E - k) \cos \theta_{MS/2}/c)^2 - (mc)^2} - k/c \quad (4)$$

where $\theta_{MS/2}$ is the multiple scattering in half the formation length, $E_s/E\sqrt{l_f/2X_0}$, where $E_s = m\sqrt{4\pi\alpha} = 21$ MeV, and X_0 is the radiation length. Scattering after the interaction is for electron energy $E - k$. This leads to a quadratic in l_f :

$$l_f = \frac{2\hbar E(E - k)}{km^2c^3(1 + E_s^2l_f/m^2c^4X_0)} = l_{f0} \left[1 + \frac{E_s^2l_f}{m^2c^4X_0} \right]^{-1}. \quad (5)$$

If multiple scattering is small, this reduces to Eq. (3). When multiple scattering dominates

$$l_f = \sqrt{\frac{2\hbar c E(E - k)X_0}{E_s^2k}} = l_{f0} \sqrt{\frac{kE_{LPM}}{E(E - k)}}. \quad (6)$$

where E_{LPM} is a material dependent constant, given by $E_{LPM} = m^4c^7X_0/2\hbar E_s^2 \approx 3.85$ TeV/cm X_0 . For lead, $E_{LPM} = 2.2$ TeV, while for water $E_{LPM} = 139$ TeV and for sea level air $E_{LPM} = 117$ PeV.

Since the formation length is the maximum distance over which the bremsstrahlung amplitude add coherently, the bremsstrahlung amplitude is proportional to the formation length, so the suppression factor is

$$S = \frac{d\sigma/dk}{d\sigma_{BH}/dk} = \frac{l_f}{l_{f0}} = \sqrt{\frac{kE_{LPM}}{E(E - k)}} \quad (7)$$

and the $dN/dk \sim 1/k$ found by Bethe and Heitler changes to $dN/dk \sim 1/\sqrt{k}$.

A similar effect occurs for pair production, where the produced electron and positron can multiple scatter. The two effects are closely related, as is shown in Fig. 1, and this relationship can be used to relate the bremsstrahlung and pair creation formation lengths and cross sections. For pair production

$$l_{f0} = \frac{2\hbar E(k - E)}{m^2c^3k}; \quad (8)$$

the corresponding suppression is

$$S = \sqrt{\frac{kE_{LPM}}{E(k - E)}}. \quad (9)$$

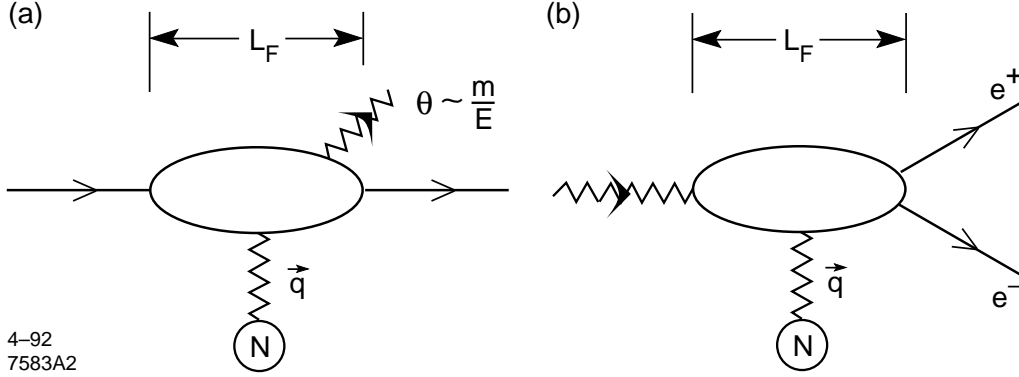


FIGURE 1. Schematic Representation of bremsstrahlung and pair conversion, showing the formation zone.

This calculation has several limitations. The semi-classical approach may fail for $k \sim E$. The calculation neglects the statistical nature of multiple scattering, instead treating it deterministically. And, it neglects many niceties like the large non-Gaussian tails on Coulomb scattering and electron-electron inelastic scattering.

Migdal developed a more sophisticated approach which avoided many of these problems [2]. He treated the multiple scattering as diffusion, calculating the average radiation for each trajectory, and allowing for interference between nearby collisions. He found the cross section for bremsstrahlung is

$$\frac{d\sigma_{\text{LPM}}}{dk} = \frac{4\alpha r_e^2 \xi(s)}{3k} \{y^2 G(s) + 2[1 + (1 - y)^2] \phi(s)\} Z^2 \ln \left(\frac{184}{Z^{1/3}} \right). \quad (10)$$

where $G(s)$ and $\phi(s)$ are the solutions to differential equations, given by [3]

$$\phi(s) = 1 - \exp \left[-6s[1 + (3 - \pi)s] + s^3/(0.623 + 0.796s + 0.658s^2) \right] \quad (11)$$

$$\psi(s) = 1 - \exp \left[-4s - 8s^2/(1 + 3.96s + 4.97s^2 - 0.05s^3 + 7.5s^4) \right] \quad (12)$$

$$G(s) = 3\psi(s) - 2\phi(s). \quad (13)$$

where

$$s = \frac{1}{2} \sqrt{\frac{E_{\text{LPM}} k}{E(E - k) \xi(s)}}. \quad (14)$$

For $k \ll E$, $s \sim 1 / \langle \gamma \theta_{MS} \rangle$. For $s \gg 1$, there is no suppression, while for $s \ll 1$, the suppression is large. $\xi(s)$ accounts for the increase in radiation length as photon emission drops. Migdal's solution for s and $\xi(s)$ is recursive, because s depends on $\xi(s)$. The recursion can be avoided by defining [3]

$$s' = \frac{1}{2} \sqrt{\frac{E_{\text{LPM}} k}{E(E - k)}}. \quad (15)$$

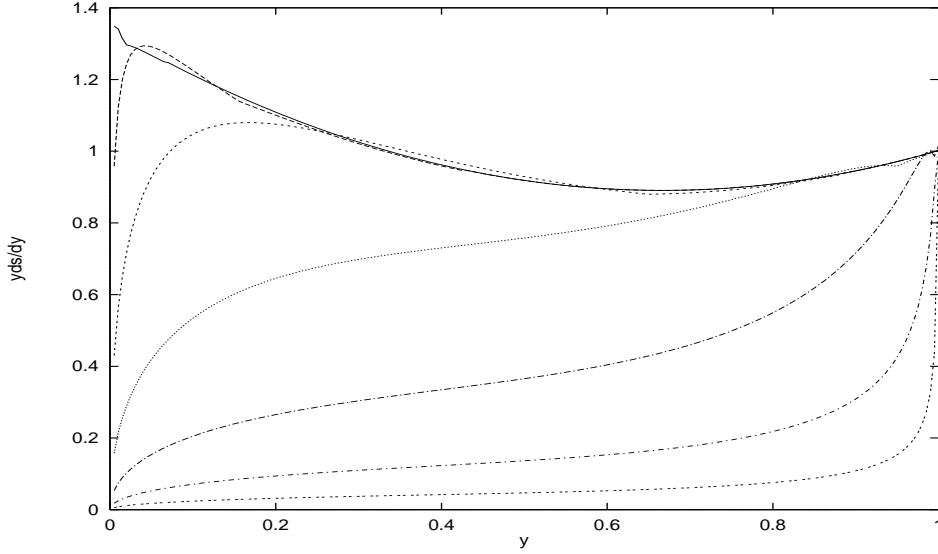


FIGURE 2. $y d\sigma_{LPM}/dy$ for bremsstrahlung as a function of y for various electron energies in lead ($E_{LPM}=2.2$ TeV), showing how the spectral shape changes. Electrons of energies 10 GeV, 100 GeV, 1 TeV, 10 TeV, 100 TeV, 1 PeV and 10 PeV are shown. The upper curve (solid line) is for $E = 10$ GeV, and the emission drops as energy rises.

This is possible because ξ depends only logarithmically on s ; a modified formulae for ξ depends only on s' :

$$\xi(s') = 2 \quad (s' < \sqrt{2}s_1) \quad (16)$$

$$\xi(s') = 1 + h - \frac{0.08(1-h)[1-(1-h)^2]}{\ln \sqrt{2}s_1} \quad (\sqrt{2}s_1 < s' \ll 1) \quad (17)$$

$$\xi(s') = 1 \quad (s' \geq 1) \quad (18)$$

where $h = \ln s' / \ln(\sqrt{2}s_1)$. In the strong suppression limit, $s \rightarrow 0$, $G(s) = 12\pi s^2$ and $\phi(s) = 6s$. With these approximations, the semi-classical $d\sigma/dk \sim 1/\sqrt{k}$ scaling is recovered, albeit with a different coefficient.

Fig. 2 shows how the LPM effect reduces $y d\sigma/dy$ ($y = k/E$) for electrons in a lead target. The 10 GeV electron curve is very close to the Bethe-Heitler prediction; in the absence of suppression, this curve would hold for all electron energies. As the electron energy rises, emission drops. At the highest electron energies, photons with $k \ll E$ are almost completely suppressed. For $E^2/E_{LPM} < k < 1.3E^2/E_{LPM}$, the Migdal curve rises slightly above the unsuppressed; this is a consequence of either the approach or the approximations Migdal used.

Fig. 3 shows how the pair production cross section is reduced. Compared with bremsstrahlung, pair production suppression sets in at higher energies. Symmetric pairs are suppressed the most; in the extremely high energy limit, one of the produced electrons takes almost all of the photon energy. So, where the LPM effect is extremely strong, an electromagnetic shower becomes a succession of interactions

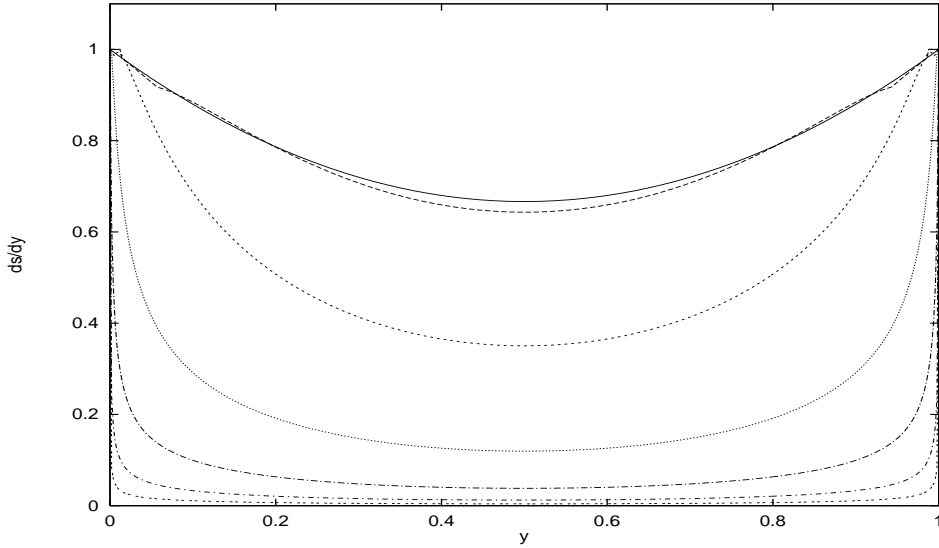


FIGURE 3. $d\sigma_{LPM}/dy$ for pair production in lead, as a function of y for various photon energies, showing how the spectral shape changes. The solid line is for $k = 1$ TeV, and the cross sections drop with energy; the other curves are for photons of energies 1 TeV, 10 TeV, 100 TeV, 1 PeV, 10 PeV, 100 PeV and 1 EeV.

where an electron emits a bremsstrahlung photon that takes almost all of the electrons energy, followed by a very asymmetric pair conversion, producing an electron or positron with almost all of the energy of the initial lepton.

Two metrics for suppression effects in showers are the electron energy loss (dE/dx) and photon conversion cross section. Fig. 4 shows how these two markers change with energy in a lead target. As the particle energy rises above E_{LPM} (2.2 TeV for lead), the energy loss and conversion cross section fall, with bremsstrahlung affected at lower energies than pair conversion.

The LPM effect was studied experimentally by the SLAC E-146 collaboration, who sent 8 and 25 GeV electrons through thin (0.07 % to 6% of X_0) targets of materials ranging from carbon to gold. Fig. 5 shows their data for carbon [4], the material that is closest to air. Both LPM and dielectric suppression are needed to explain the data.

Since E-146, there have been a number of additional calculations of bremsstrahlung with multiple scattering, using a variety of different approaches [5–8]. Several calculations have showed that, the non-Gaussian tail of large angle Coulomb scatters introduces additional term into the cross section; in the limit of large suppression [6–8]

$$S = \sqrt{\frac{kE_{LPM}}{E(E-k)} \log\left(\frac{E(E-k)}{kE_{LPM}}\right)} \quad (19)$$

This will reduce the magnitude of suppression in extreme conditions. Inelastic

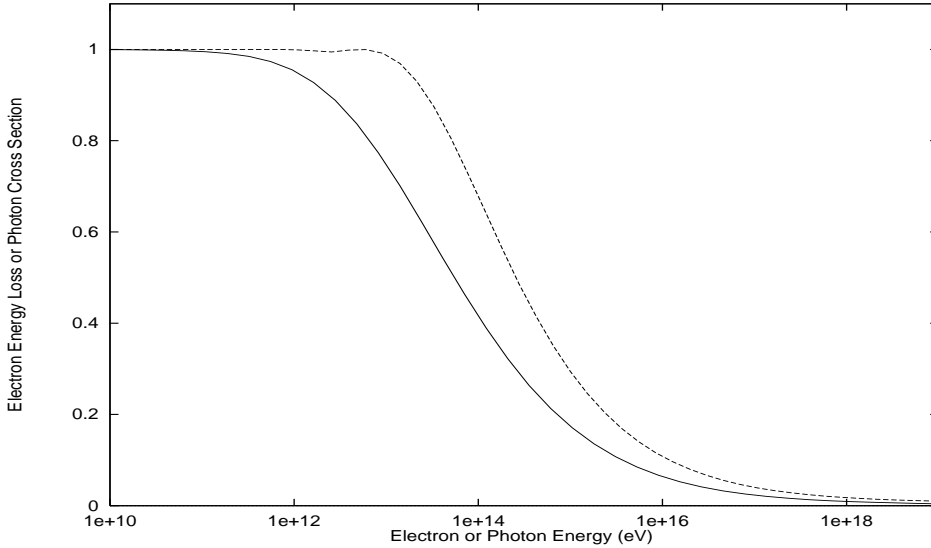


FIGURE 4. The reduction in electron energy loss ($\int_0^E (kdN/dk)dk$) due to the LPM effect (solid line) and in the photon conversion cross section (dashed line) due to the LPM effect in a lead target. The LPM effect turns on at higher energies for photons.

interactions, involving the atomic electrons should be treated separately from the elastic nuclear interactions, and a different potential should be used [6,8]. This may explain the poor agreement observed by E-146 between the data and the Migdal calculations for their light carbon and aluminum targets, especially for the 25 GeV data, around $k = E^2/E_{LPM}$. In light of these results, calculations based on Migdal's formulae should be treated with caution, especially for light targets like air, where the inelastic form factor is important.

B Dielectric Suppression

Dielectric suppression occurs because photons produced in bremsstrahlung can interact with the atomic electrons in the medium by forward Compton scattering [9]. The photon wave function acquires a phase shift depending on the dielectric constant of the medium $\epsilon(k) = 1 - (\hbar\omega_p)^2/k^2$ where ω_p is the plasma frequency of the medium. With this substitution, the photon momentum (k/c) in Eq. (1) becomes $\sqrt{\epsilon}k/c$, and q_{\parallel} acquires an additional term $(\hbar\omega_p)^2/2ck$. This leads to a reduced l_f , and a suppression factor

$$S = \frac{k^2}{k^2 + (\gamma\hbar\omega_p)^2}. \quad (20)$$

This effect only applies for small y , $y < y_{die} = \omega_p/m$. For typical solids, $\omega_p \sim 60$ eV, so $y_{die} \sim 10^{-4}$. For $y < y_{die}$, the photon spectrum becomes $d\sigma/dk \sim k$, suppressing

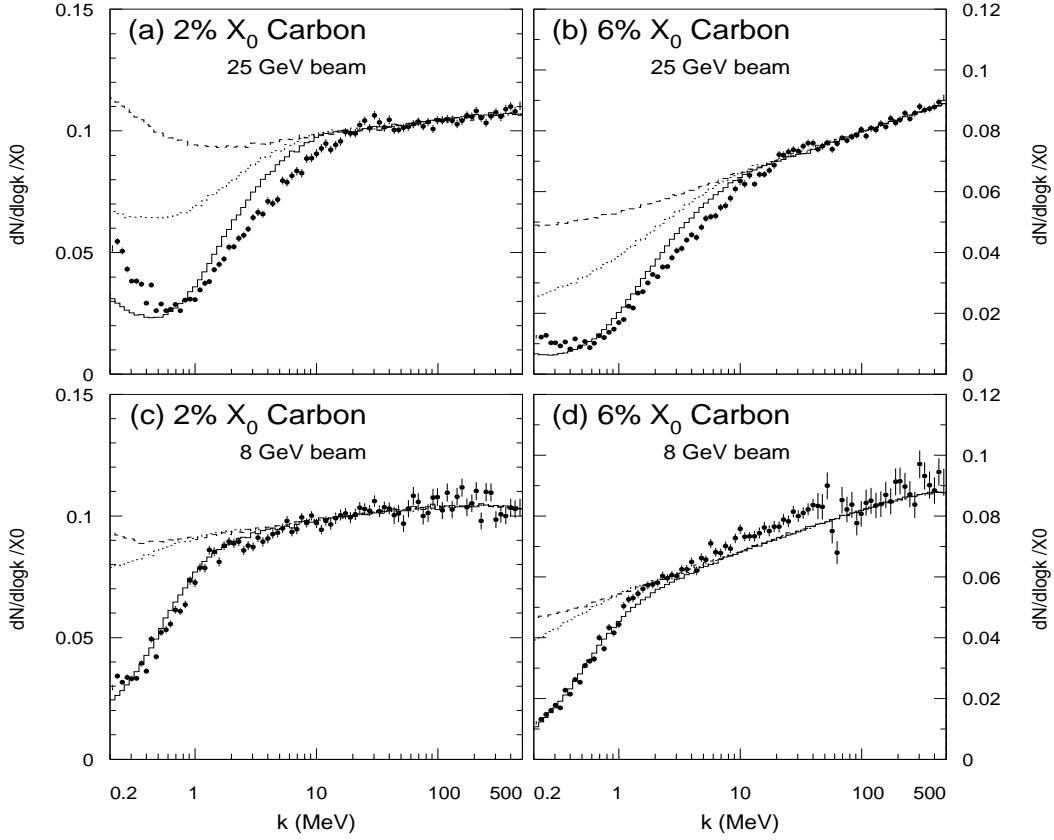


FIGURE 5. Comparison of data from SLAC-E-146 with Monte Carlo predictions for 200 keV to 500 MeV photons from 8 and 25 GeV electrons passing through 2% and 6% X_0 thick carbon targets. The cross sections are $dN/d(\log k)/X_0$ where N is the number of photons per energy bin per incident electron, for (a) 2% X_0 carbon and (b) 6% X_0 carbon targets in 25 GeV electron beams, while (c) shows the 2% X_0 carbon and (d) the 6% X_0 carbon target in the 8 GeV beam. Monte Carlo predictions are shown for LPM plus dielectric suppression (solid line), LPM suppression only (dotted line) and Bethe-Heitler (dashed line); all include transition radiation.

the emission by $(\gamma\hbar\omega_p)^2/k^2$. The effect is also clearly apparent in the E-146 data in Fig. 5.

C Suppression of Bremsstrahlung by Pair Creation, and vice-versa

As Landau and Pomeranchuk pointed out, when l_{f0} becomes as long as X_0 , then partially created photons can be pair create, destroying the coherence [1]. A simple calculation of this effect can be done by limiting l_f to a maximum of $1X_0$ [10]. This suppression is visible (stronger than LPM and dielectric suppression) for

$$E > E_p = \frac{2X_0\omega_p E_s}{\hbar c}. \quad (21)$$

For $E > E_p$, there is a 'window' in k where this mechanism applies: $k_{p-} = X_0\omega_p^2/2\hbar c < k < k_{p+} = 2\hbar c E(E-k)/(X_0 E_s^2)$. In this region, the photon spectrum is suppressed by k , and $d\sigma/dk$ is constant. For $k < k_{p-}$, dielectric suppression dominates, while for $k > k_{p+}$, the LPM effect is dominant. E_p is 1.6 PeV in water or ice, and 42 PeV for air at sea level. The E_p s are so similar because the variation in X_0 and ω_p partially offset each other. In sea level air, the 'window' is $331 \text{ MeV} < k < 3.0 \times 10^{-24} E^2$ (with E in eV).

There should be a similar effect where a partially produced electron or positron emits a bremsstrahlung photon. This possibility limits the coherence over l_{f0} . The strength of this suppression has not yet been calculated, but it should be comparable to that for pair production suppressing bremsstrahlung.

This approach is overly simplistic. The 'hard cutoff' in l_f should be replaced by a probabilistic approach, where the photon interaction probability depends on the distance travelled. And, other suppression mechanisms will also be in effect, the radiation length will be longer than the naive $1X_0$. An accurate calculation should include the interplay between the two reactions to arrive at an overall effective shower distance. Still, the above equation gives a reasonable estimate of when this effect needs to be considered.

Fig. 6 summarizes these results, and shows that a 'simple' bremsstrahlung photon spectrum can have several different slopes for different photon energies.

D Magnetic Suppression

An external magnetic field can also suppress bremsstrahlung and pair creation. The bending caused by an external field acts just as does multiple scattering. The difference is that the magnetic field bending is quite deterministic, while the scattering angles are randomly distributed. The magnetic bending angle is $\theta_B = \Delta p/p = eBl_f \sin(\theta_B)/E$ where B is the magnetic field and θ_B is the angle between the field and the electron trajectory. Emission is reduced if $\theta_B > 1/\gamma$; this

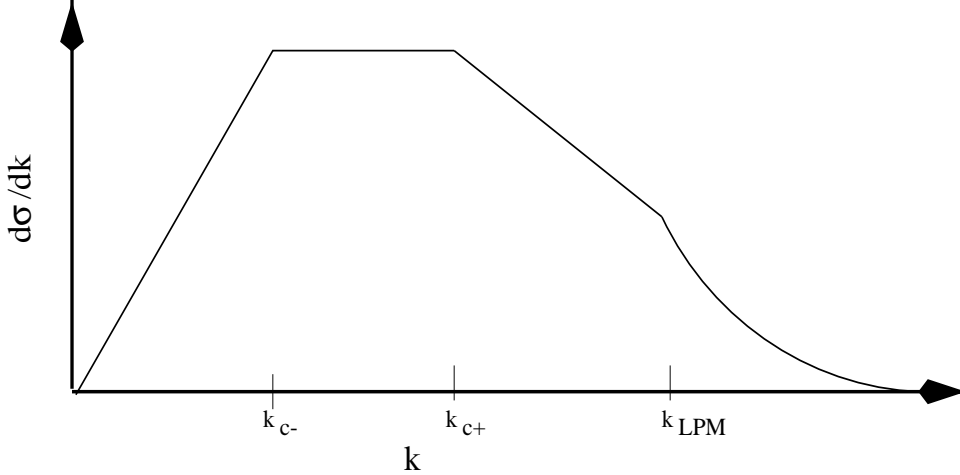


FIGURE 6. Schematic view of bremsstrahlung $d\sigma/dk$ when several suppression mechanisms are present. Below k_{c-} , dielectric suppression dominates. Between k_{c-} and k_{c+} , suppression due to pair creation is dominant. Between k_{c+} and $k_{LPM} = E^2/E_{LPM}$, the LPM effect is most important, while above k_{LPM} the Bethe-Heitler spectrum is present. For $E < E_p$, pair creation suppression disappears and LPM suppression connects with dielectric suppression.

happens for $y < 2\gamma B \sin(\theta_B)/B_c$, where $B_c = m^2 c^3/\hbar$ is the critical field strength [11].

The magnitude of the suppression can be found using an approach similar to that used by Landau and Pomeranchuk for multiple scattering. Because $\theta_B \sim l_f$, while $\theta_{MS} \sim \sqrt{l_f}$ the energy dependence is different. With the definition $E_B = mB_c/B \sin(\theta_B)$, the suppression factor is [12]

$$S = \left[\frac{kE_b}{E(E-k)} \right]^{2/3}. \quad (22)$$

A magnetic field will also bend pair produced electrons and positrons. The same equation holds, except that $k - E$ replaces $E - k$. For a particle trajectory perpendicular to Earth's ~ 0.5 Gauss field, $E_B \sim 45$ EeV. So, for cosmic rays with energies above 10^{20} eV, magnetic suppression must be considered.

E Emission Angles

Besides reducing the interactions rates, these mechanisms also increase the angular spread of electromagnetic showers. When bremsstrahlung and pair creation occur with a large opening angle, the formation length is shortened. For bremsstrahlung

$$l_{f0} = \frac{2\hbar E(E-k)}{m^2 c^3 k(1 + \gamma^2 \theta_\gamma^2)} \quad (23)$$

where θ_γ is the angle between the photon and the electron trajectory. When θ_γ is included in the calculations, the average emission angle rises from $\theta_\gamma \sim 1/\gamma$ to $\theta_\gamma \sim 1/S\gamma$. If S is small enough, this spreading can dominate over multiple scattering in determining the angular spreading of the shower. If the scattering is taken over $1/2X_0$ (assuming 1 interaction per X_0 , and half the particles are charged and hence subject to multiple scattering), this occurs for roughly $S < 0.05$. Most calculations of air and water showers do not include this angular spreading. It is likely to be most important for calculations for radio emission from showers in air and ice [13].

II SUPPRESSION IN SHOWERS

Suppression mechanisms can affect showers by slowing their development, effectively increasing the radiation length. Because they all work by reducing l_f , the effects do not add; instead, q_{\parallel} must be summed, and the total suppression calculated. Usually, multiple scattering is the most significant cause of suppression, so it will be the focus of this section.

The effective increase in radiation length due to multiple scattering can be seen in Figs. 4; it shows how the area under the curve in Figs. 2 and 3 drops as the incident particle energy rises. For bremsstrahlung, energy loss is halved for electrons with $E = 22E_{LPM}$, while the pair production cross section is halved for $k = 100E_{LPM}$. Then, the radiation length in the first generation of the shower doubles; succeeding generations will show smaller effects.

However, the effects go beyond simply lengthening showers. Because soft photon bremsstrahlung is the first reaction to be affected, the number of interactions will decrease more rapidly than the electron energy loss. So, the initial part of a shower will consist almost entirely of a few high energy particles, without an accompanying 'fuzz' of lower energy particles. The initial shower development depends on a much smaller number of interactions. For example, a 25 GeV electron in sea level air will emit about 14 bremsstrahlung photons per X_0 , while a 10^{17} eV electron will emit only 3. It is worth noting that, these numbers are naturally finite because dielectric suppression eliminates the infrared divergence. Pair production is similar; the pairs become increasingly asymmetric. The higher energy lepton from a 25 GeV photon pair conversion takes an average of 75% of k ; for a 10^{19} eV photon, the average is more than 90%.

Because of this, shower to shower fluctuations become much larger. Misaki studied shower development in lead and standard rock. For $E \gg E_{LPM}$ he found that the position of shower maximum was shifted to larger depths, and that the position of shower maximum varied greatly from shower to shower, and that the shower to shower variations overshadowed the average shower development [14].

In the limit $E \gg E_{LPM}$, the initial part of an air shower becomes a succession of asymmetric pair production, where the higher energy of the pair loses most of its energy to a single bremsstrahlung photon, re-starting the process. In short, the

paradigm that successive generations of air showers have twice as many particles with half as much energy as the current generation fails completely.

III AIR SHOWERS

The composition of the highest energy cosmic rays is still a mystery. This article will consider two possibilities: protons (the most popular) and photons. In both cases, we will take 3×10^{20} eV as a standard energy. For incoming heavy ions, the effects are greatly reduced because of the lower per particle energy, and neutrons can be treated as protons. Because these are toy models, the likely possibility of the photon pair converting in the earth's magnetic field will be neglected.

Most current works have considered proton initiated showers. There has been disagreement as to whether the LPM effect is important in air showers. Capdevielle and Atallah found that it had a large effect on 10^{19} eV and 10^{20} eV showers [15]. However, Kalmykov, Ostapchenko and Pavlov found a much smaller effect; for a 10^{20} eV incident proton, the number of electrons at shower maximum decreased by 5%, while the position of shower maximum shifted downward by 15 ± 2 g/cm² [16]. This shift is less than the error on a typical measurement of shower maximum in a single shower, but it can have a significant effect on composition studies. Of course, as experiments probe higher energies, suppression becomes more important. None of these authors considered the effects of fluctuations or other suppression mechanisms.

Air showers studies are complicated by the fact that density, and hence E_{LPM} and E_p depend on altitude and temperature. Ignoring temperature changes, pressure decreases exponentially with altitude, with scale height 8.7 km. For showers, it is convenient to work with column depth measured in g/cm². In an isothermal model, then $E_{LPM} = 117 \text{ PeV}(A_0/A)$, where A is the column depth and A_0 is ground level, 1030 g/cm². Temperature will modify the relationship; with a temperature correction this E_{LPM} is 2.25 EeV at 36 g/cm² ($1 X_0$) depth, and 1 EeV at 90 g/cm² (1 hadronic interaction length, Λ). Neglecting temperature, $y_{die} = 1.3 \times 10^{-6} A/A_0$. For pair creation suppression, $E_p = 42 \text{ PeV} \sqrt{(A_0/A)}$. The corresponding photon window is $331 \text{ MeV} < k < 3.0 \times 10^{-24} E^2(A_0/A)$. The two window 'edges' have different A dependencies because all three mechanisms have a different dependence on ω_p and X_0 .

Incoming photons react by pair production, while protons interact hadronically. A central hadronic collision will produce a shower of several hundred pions; the neutral pions will decay to photons. The highest energy π^0 will have a rapidity near to the incoming proton, and their decay photons will have energies around 2×10^{19} eV. Many diffractive processes, such as Δ production can produce photons with similar energies. Overall, photons from central interaction will have an average energy of about 2×10^{17} eV.

Although a complete Monte Carlo simulation is required to understand the effects of suppression in air showers, simple calculations can provide some indications

where it matters, and should differentiate between the results of Capdevielle and Atallah and Kalmykov and collaborators. Because E_{LPM} decreases with depth, in concert with the average particle energy, suppression mechanisms can actually become stronger as one moves deeper in the atmosphere. The solid curve in Fig. 7 shows E_{LPM} as a function of altitude. The dashed curve shows the average particle energy, for an idealized Bethe-Heitler shower from a 3×10^{20} eV photon. In each successive radiation length, there are twice as many particles with half the energy. The curve with the short dashes shows a similar cascade, from a 2×10^{19} eV photon starting at 1A. The electromagnetic interactions at a given depth are determined by the ratio of the two curves, which gives E/E_{LPM} . For the photon case, the maximum suppression occurs around 75 g/cm^2 , where $E \sim 80E_{LPM}$. Electron dE/dx is reduced about 80%, and pair production cross section is down by 60%; the radiation length has more than doubled. For the hadronic case, the effect is smaller, and, of course, these high energy photons are only a small portion of the total shower. On the other hand, hadronic interactions are only partially inelastic, and the proton may carry a significant fraction of its momentum deeper in the atmosphere, where suppression is larger. Because of the large variations in energy deposition depths, it is difficult to give more quantitative estimates.

This model underestimates the effect of suppression, because, with suppression shower development is slower than the idealized model, further increasing the amount of suppression in the next stage. However, it does show that suppression is important in photon shower, and in at least parts of proton initiate showers. The effect is clearly smaller than that predicted by Capdevielle and Atallah, but is consistent with Kalmykov and collaborators.

Beyond the affect on average showers, fluctuations must be considered. because the cosmic ray energy spectrum falls as $dN/dE \approx 1/E^3$, it is important to understand the tails of the energy resolution distribution; without accurate simulations, showers whose energy is overestimated can easily skew the measured spectrum.

Fluctuations can affect both ground based arrays as well as air fluorescence detectors that optically measure the shower development. For ground based arrays, suppression can change the relative position of shower maximum and the detector array. Although a sea level detector is near shower maximum for 10^{20} eV vertically incident proton showers, for non-vertical showers, where the detector is deeper, it may be significantly behind shower maximum. The angular spreading discussed in Subsection IE must also be considered.

Air fluorescence detectors will observe far fewer particles in the early stages of the shower than current simulations indicate. LPM, dielectric and pair creation suppression must all be considered. Although LPM suppression affects the widest range of energies, the other mechanisms produce a larger reduction in cross section where they operate. For $E > E_p$, for example, dielectric suppression will reduce the number of bremsstrahlung photons with $k < 331 \text{ MeV}$ by two orders of magnitude. Pair creation suppression is more energy dependent, but, for example, at 200 g/cm^2 depth, emission of 10^{10} eV photons from 10^{16} eV electrons will be reduced by a factor of 10. Monte Carlo simulations are required to find the actual shower profile, but

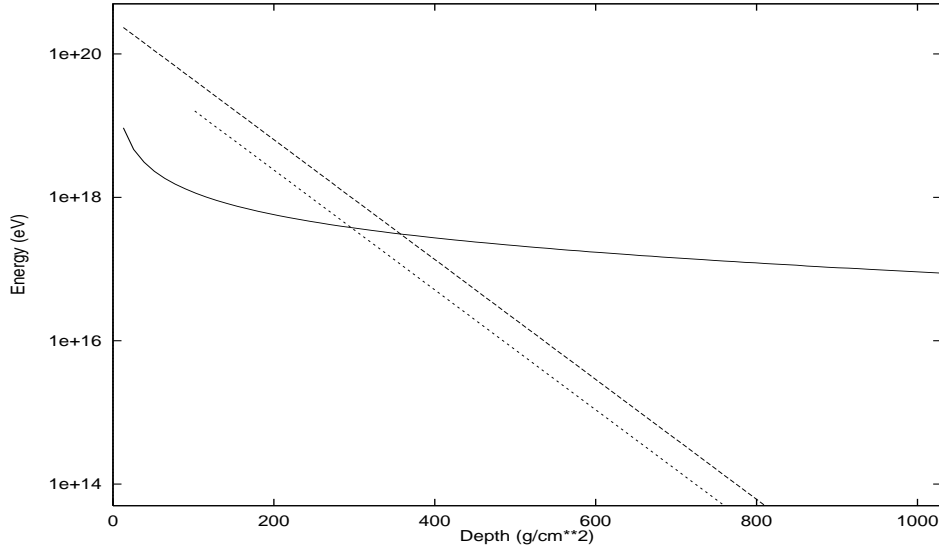


FIGURE 7. E_{LPM} (solid line), average particle energy for a 3×10^{20} eV photon shower (dashed line) and average particle energy for a 2×10^{19} eV photon created at 1Λ (short dashes). At altitudes where the average particle energy is larger than E_{LPM} , suppression is important; with the ratio of the two energies determining the degree of suppression.

the initial stages of the shower will be much less visible than current simulations indicate; neither the profiles produced by Capdevielle and Atallah nor by Kalmykov will be accurate.

Even relatively late in the shower, there will be a reduction in the number of low energy particles. For example, where the average particle energy is $\sim 10^{13}$ eV, LPM suppression will reduce the number of photons below ~ 500 MeV. So, there can be measurable effects even relatively close to shower maximum. if a particle counting detector is too far above shower maximum, then it may underestimate the size of the shower.

Another way to visualize how suppression works is to consider the probability of photons penetrating deep into the atmosphere. Because, for a given photon energy, suppression increases with depth, high energy photons have a non-negligible probability of penetrating deep into the atmosphere. This can drastically change the development of photons showers. For proton showers, it can create small, dense subshowers within the main shower. Fig. 8 shows the interaction probability as a function of depth for a 3×10^{20} eV vertically incident photon. The solid and dashed curves show the LPM and Bethe-Heitler cases respectively. With Bethe-Heitler interaction probabilities, essentially all of the photons have interacted by $3X_0$ in depth, while with LPM interaction probabilities, the photon has a 7% chance of surviving to $10X_0$.

For protons, the effect is smaller, The other curves in Fig. 8 are for a 2×10^{19} eV photon, produced by a hadronic interaction at 1Λ in depth. With Bethe-Heitler (short dashes), almost all have interacted by $6 X_0$, while with LPM (dots) cross

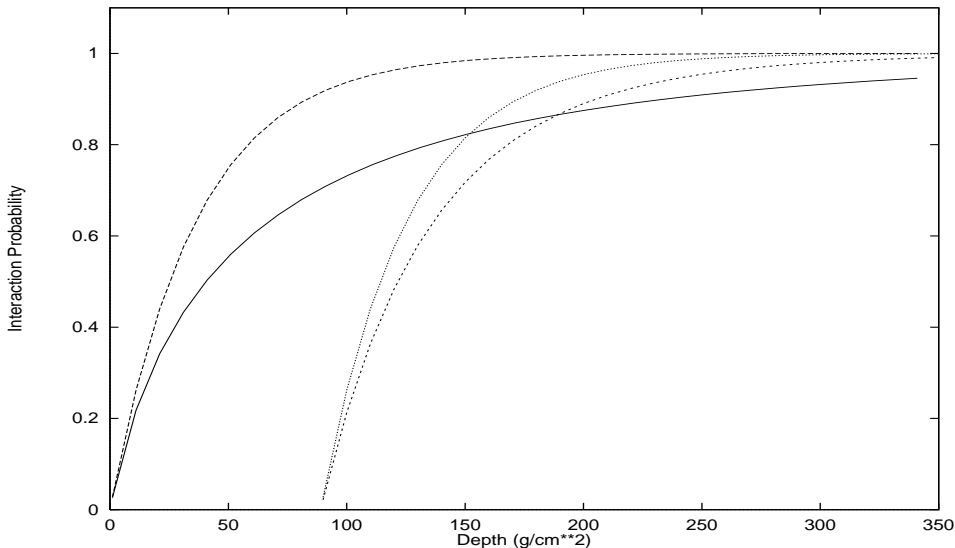


FIGURE 8. Interaction probability for photons from cosmic rays, as a function of depth in the atmosphere. The solid and dashed line show the interaction probability for a 3×10^{20} eV photon incident on the top of the atmosphere for LPM and Bethe-Heitler interaction probabilities respectively. The short dashed and dotted lines show the interaction probability for a 2×10^{19} eV photon produced in an interaction at a depth of 1Λ , also for LPM and Bethe-Heitler interactions respectively.

sections, it has a 1.2% chance of surviving to $10X_0$. The effect on the average shower is small, but, because of the steeply falling spectrum, it is necessary to consider even relatively atypical showers.

Not considered here is magnetic suppression, which can dominate over other mechanisms for interactions in the upper 3 g/cm^2 of the atmosphere.

IV CONCLUSIONS AND ACKNOWLEDGEMENTS

Multiple scattering, the dielectric of the medium, bremsstrahlung and pair production themselves and external magnetic fields can suppress bremsstrahlung and pair production, with bremsstrahlung of low energy photons the most subject to suppression. Suppression also broadens the angular spread of emitted bremsstrahlung photons and produced pairs.

For energetic enough particles, these mechanisms reduce electron dE/dx and photon pair production cross sections. When this happens, electromagnetic showers are lengthened, and shower to shower fluctuations become much larger. When suppression gets very large, then the shower angular development can be dominated by interactions, rather than multiple scattering.

The importance of suppression in air showers depends on the incident particle type and energy. If the incoming particles are photons, then at 3×10^{20} eV, the

effects are large. For 3×10^{20} protons, the effects on the average shower is smaller, but the effects of fluctuations may be considerable, particularly when particular detector are included. As experiments probe to higher energies, of course, the effects will grow larger.

The calculations presented here show the need for a complete Monte Carlo, including all relevant suppression mechanisms, in order to correctly determine the shower profile for showers with energies much above 10^{20} eV.

I would like to thank my E-146 collaborators for many useful discussions. This work was supported by the USDOE under contract number DE-AC-03-76SF00098.

REFERENCES

1. Landau, L.D and Pomeranchuk, I.J., Dokl. Akad. Nauk. SSSR **92** 535 (1953); Dokl. Akad. Nauk. SSSR **92**, 735. These papers are available in English in *The Collected Papers of L. D. Landau*, Pergamon Press, 1965.
2. Migdal, A. B., Phys. Rev. **103**, 1811 (1956).
3. Stanev, T. *et al.*, Phys. Rev. D **25**, 1291 (1982).
4. Anthony, P. *et al.*, Phys. Rev. Lett. **75**, 1949 (1995); Phys. Rev. Lett. **76**, 3550 (1996); Phys. Rev. **D56**, 1373 (1997).
5. Blankenbecler, R. and Drell, S., Phys. Rev. **D53**, 6285 (1996).
6. Zakharov, B. G., JETP Lett. **64**, 781 (1996).
7. Baier, R., Dokshitzer, Yu. L, Mueller A. H. and Schiff, D, Nucl. Phys. **B478**, 57 (1996).
8. Baier, V.N., and Katkov, V.M., hep-ph/9709214, Sept., 1997.
9. Ter-Mikaelian, M. L., Dokl. Akad. Nauk. SSR **94**, 1033 (1953); *High Energy Electromagnetic Processes in Condensed Media*, John Wiley & Sons, 1973.
10. Galitsky, V.M. and Gurevich, I.I., Il Nuovo Cimento **32**, 396 (1964).
11. Klein, S. R. *et al.*, in *Proc. XVI Int. Symp. Lepton and Photon Interactions at High Energies*, Eds. P. Drell and D. Rubin, AIP Press, 1993.
12. Klein, S. R., to be published.
13. Alvarez-Muniz, J. and Zas, E., preprint astro-ph/9706064.
14. Misaki, A., Nucl. Phys. B (Proc. Suppl.) **33A,B**, 192. (1993).
15. Capdevielle, J. N. and Atallah, R., Nucl. Phys. B (Proc. Suppl.), **28B**, 90 (1992).
16. Kalmykov, N. N., Ostapchenko, S. S. and Pavlov, A. I., Phys. Atomic Nuclei **58**, 1728 (1995).